Ordered polyelectrolyte assembly at the oil–water interface

Daniel K. Beaman, Ellen J. Robertson, and Geraldine L. Richmond[1]

Department of Chemistry, University of Oregon, Eugene, OR 97403

Contributed by Geraldine L. Richmond, January 9, 2012 (sent for review October 14, 2011)

Polyelectrolytes (PEs) are widely used in applications such as water purification, wastewater treatment, and mineral recovery. Although much has been learned in past decades about the behavior of PEs in bulk aqueous solutions, their molecular behavior at a surface, and particularly an oil–water interface where many of their applications are most relevant, is largely unknown. From these surface spectroscopic and thermodynamics studies we report the unique molecular characteristics that several common polyelectrolytes, poly(acrylic acid) and poly(methylacrylic acid), exhibit when they adsorb at a fluid interface between water and a simple insoluble organic oil. These PEs are found to adsorb to the interface from aqueous solution in a multistepped process with a very thin initial layer of oriented polymer followed by multiple layers of randomly oriented polymer. This additional layering is thwarted when the PE conformation is constrained. The adsorption/desorption process is highly pH dependent and distinctly different than what might be expected from bulk aqueous phase behavior.

macromolecular assembly | surface spectroscopy | water surfaces | hydrophobic surfaces | surfactants

The junction between an insoluble oil and an aqueous phase provides a truly unique environment for adsorption and assembly of ions, surfactants, and macromolecules, processes that we are only beginning to understand. The forces that drive adsorption at this interface are often described in simple "water hating" and "water seeking" terms when, in fact, the adsorption process can have many complex competing interactions. This is certainly true for polymeric macromolecules with their hydrophobic backbones that coil and bend into a multitude of conformations, and the fickle hydrophilic functional groups whose characteristics can vary widely depending upon the aqueous phase composition. Unlike a simple alkyl surfactant that can be satisfied by submerging its polar headgroup in the aqueous portion of the interface while stretching its tail into the oily phase, a charged macromolecule with its analogous tails that compose the backbone is more constrained. The juxtaposition of the hydrophobic and hydrophilic regions of such macromolecules makes predictability of their behavior at a liquid–liquid interface difficult. Polyelectrolytes (PEs) are a case in point. The density and charge of various polar groups dispersed on a largely hydrophobic PE backbone, the tendency for many PEs to form complicated coiled and extended conformations, and the PE's solubility in either the oil or aqueous phase can all be factors in determining whether a PE will initially adsorb and foster subsequent layers to adsorb to the interfacial region.

This study is one of the first to explore on a molecular level the adsorption and assembly of several common polyelectrolytes at a liquid–liquid interface. The results demonstrate the unique multistep manner with which various PEs assemble at this interface and the intrinsic properties of the oil–water interface itself that drive the initial assembly of a PE layer that is highly oriented. The role that the polymer charge, polymer backbone, and solution composition play in this first and subsequent interfacial layer is also articulated.

Two related PEs have been chosen for this study: poly(acrylic acid) (PAA) and poly(methacrylic acid) (PMA). Both of these PEs are carboxylate containing polyelectrolytes that are prevalent in many commercial and technological applications. These PEs also serve as models for humic substances, which are composed of complex organic macromolecules with carboxylate moieties (1–3), and as model systems for understanding more complex biological systems such as binding to DNA and proteins as well as in studies of tissue substitutes (4, 5). Although the behavior of these PEs has been widely studied for bulk liquids, their molecular behavior at a surface, particularly at a liquid–liquid interface where their applications are most relevant, is largely unknown. In fact, the few molecular-level studies that do examine PE behavior at any liquid surface presume that the addition of surfactant is necessary to induce surface adsorption, contrary to what is observed here for PAA or PMA.

PAA consists of a hydrocarbon backbone on which carboxylate groups are bonded on alternate carbons (Fig. 1). The atactic form of PAA is used in these studies. Because of its ability to adsorb many times its weight in water, PAA's most notorious usage is in disposable baby undergarments. PMA has a similar structure but with an additional methyl group bound to the same backbone carbon as the carboxylate group. Two isomeric forms of PMA (Fig. 1) have been studied, isotactic (iPMA) where all substituents are located on the same side of the backbone, and atactic (aPMA), with the substituents randomly oriented.

Key to understanding the very ordered assembly that is observed and described in this work is the molecular nature of the platform itself, the oil–water interface. This interface has been the fascination of many since the early days of Pliny the Elder (23–79 AD), to the oil-spreading experiments of Benjamin Franklin in the countryside of New England, and to surface tension measurements of Agnes Pockels in her kitchen sink. What might have seemed a somewhat obscure interface during the emergence and growth of the field of surface science in recent decades has now suddenly come back into vogue with its growing importance in environmental remediation and oil recovery technologies (6), nanoparticle assembly (7, 8), enhanced organic synthesis (9), and its value as a model system for understanding more complex biomolecular behavior.

Our understanding of the complex assembly found in this study is aided by what we have learned over the past decade (10–12) about the molecular characteristics of this soft interface that guides the adsorption of ions and molecules. We know, for example, that weak bonding interactions between interfacial water and various hydrophobic oils is a general trait for these oil–water systems, resulting in significant molecular orientational ordering and structuring of both phases near the interfacial region (13–15). The existence of an interfacial electric field created by this structuring has been shown to facilitate the adsorption of simple electrolyte ions at the interface (15), surfactant adsorption, and also the

Author contributions: G.L.R. designed research; D.K.B. and E.J.R. performed research; D.K.B., E.J.R., and G.L.R. analyzed data; and D.K.B., E.J.R., and G.L.R. wrote the paper.

The authors declare no conflict of interest.

Freely available online through the PNAS open access option.

[1]To whom correspondence should be addressed. E-mail: richmond@uoregon.edu.

This article contains supporting information online at www.pnas.org/lookup/suppl/doi:10.1073/pnas.1200244109/-/DCSupplemental.

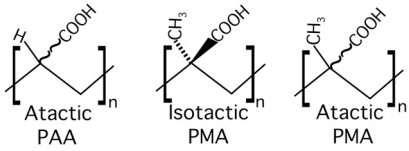

Fig. 1. Molecular structure of poly(acrylic acid), and the isotactic and atactic forms of poly(methacrylic acid).

penetration of oriented water into the organic phase (16). These studies demonstrate for the first time how all of these interfacial factors come into play in macromolecular adsorption.

Insights gained in these studies are derived from vibrational spectroscopic studies of PAA and PMA at a $CCl_4 - H_2O$ interface using total internal reflection vibrational sum frequency spectroscopy (VSFS) (17–19). The interfacial specificity of the technique (a result of $\chi^{(2)}$ only being allowed in noncentrosymmetric media) and its sensitivity to molecular moieties that have a net orientation at the interface make it an ideal probe of these systems. The use of different polarization combinations for the incident and detected beams enables molecular dipole orientation direction to be determined. Carbon tetrachloride (CCl_4) is used as the organic solvent to minimize spectral interference. These spectroscopic studies are complemented with pendant drop surface tensiometry measurements that provide a less sensitive but more unambiguous measure of adsorption (20). This is due to its sensitivity to the single variable of interfacial number density, whereas VSFS measures both orientation and number density and it is not a trivial task to deconvolute these two based on VSFS experiments alone.

Adsorption of PAA to the Oil–Water Interface

We recently observed that PAA adsorbs readily at an oil–water interface under very specific solution conditions (21). These studies expand upon this initial observation and provide a comparative case for examining if this adsorption is applicable to other PEs. When PAA is added to the aqueous phase (5 ppm, 450 kD) of a two-phase system consisting of a water (pH 2) and CCl_4, adsorption is readily apparent as the polymer progressively diffuses to the interface, causing the interfacial tension to decline to a final equilibrium value of 31 mN/m after 20 min. The presence of the polymer is confirmed in our mid-IR surface VSF measurements that detect the presence of the carbonyl vibrational mode (at 1,732 cm^{-1}) of carboxylic acids groups attached to the PAA polymer backbone (Fig. 2*A*). Because VSFS only responds to modes or molecules with a net average orientation at the surface, the strong signal observed under these polarization conditions (ssp) demonstrates that these acid groups are highly oriented with their dipoles perpendicular to the interfacial plane. There is no evidence under any polarization combination for the interfacial presence of the ionized carboxylate modes that would appear in the 1,400–1,500 cm^{-1} spectral region. This is most likely a consequence of their low number density, because the pH is well below the pK_a of PAA, but it could also be due to random orientation.

In bulk acidic aqueous solutions, PAA exists in a random coil with equally randomly oriented functional groups. The high degree of orientation of these carboxylic acid groups under acidic conditions at the interface suggests a corresponding change in the backbone of the polymer residing at the interface. Indeed, the VSF measurements in the CH stretch region confirm this to be true. As shown in Fig. 2*B* there is a dominant CH mode at 2,933 cm^{-1} with a small shoulder at 2,852 cm^{-1}. These CH modes are assigned to the asymmetric and symmetric CH_2 vibrations, respectively, and by their presence indicate that the backbone of the polymer is aligned along the interfacial plane. If it were not oriented, VSF signal would not be observed. The additional VSF response in the 3,000–3,200 cm^{-1} region corresponds

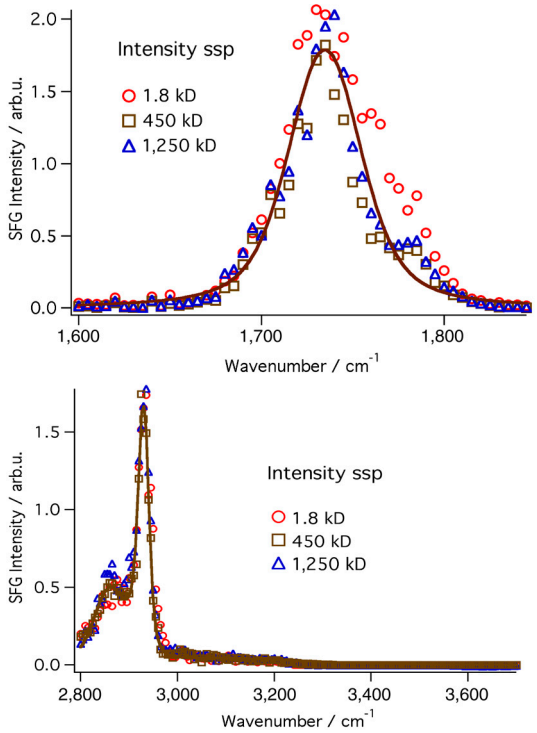

Fig. 2. VSF spectra of PAA in the carbonyl (upper) and water/CH region(lower) for three different molecular weights (1.8, 450, 1,250 kD) of the polymer. Each of the three molecular weights is observed to overlap with the others, indicating the same amount of surface coverage and orientation for each. The max intensity is representative of what is observed within one minute of setting up the oil–$PAA_{(aq)}$ interface.

to the OH stretch modes of highly coordinated water molecules in the interfacial region (16).

Variation of the molecular weight (MW) of the polymer provides new insights into the unique assembly process for PAA. Fig. 3 shows the temporal dependence in the surface tension as the MW of PAA is varied from 1.8 to 1,250 kD. The observed slower diffusion of the larger polymer to the interface is due to the increase in gyroscopic radius with the increase in molecular weight. The time to reach equilibrium ranges from approximately 12 min for 1.8 KD to 20 min for the 450-kD MW polymer. The 1,250-kD PAA interfacial tension is not observed to reach an equilibrium value even after a period of 7 h.

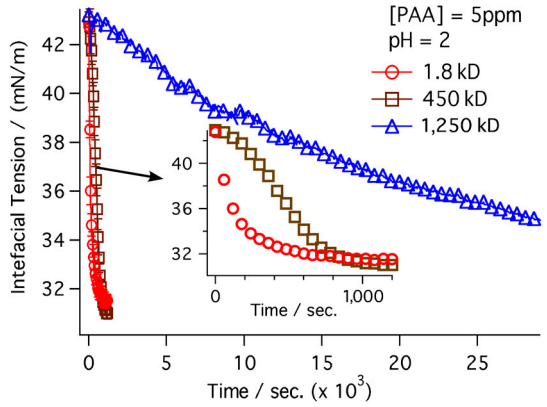

Fig. 3. Interfacial tension measurements of the three different molecular weights shown in Fig. 2 (1.8 kD, 450 kD, 1,250 kD) upon introduction of the PAA into the aqueous phase of the CCl_4-H_2O system.

Because polymer size does directly affect the rate of decline in interfacial tension, one might expect a similar variation in the VSF measurements because VSF measures sample density at the interface. Instead, neither the VSF response of the carbonyl nor the CH modes change with time after the initial spectral scans that take approximately 1 min. As noted above, spectral detection will only occur if the molecular moieties of the PAA measured have a net orientation, in this case with dipoles perpendicular to the interface. The combined results indicate that adsorption is a two-step process (21). The initial step, observable via VSFS, is a fast adsorption of the polymer into the interfacial region that equilibrates in less than a minute. The hydrophobic-hydrophilic nature of the interface and the interfacial field therein facilitates the orientational ordering of the first arriving polymer units. Calculations indicate the electric potential across the interface to be on the order of 250 mV (22), with the potential extending approximately 6–8 Å into the aqueous phase (14) before dissipating. Polymer molecules that arrive after the fast adsorption/orientation step are further removed from the field's influence and take on a more randomly coiled orientation. The result is an interfacial polymer whose outlying surface properties have very different conformational ordering than the polymer units found deeper into the interface towards the bulk aqueous phase. The field present at the interface, as discussed in previous studies (21), is clearly strong enough to align the first layer of polymer but lacks the strength to align additional polymer layers in the aqueous phase beyond those initial adsorbing layers. Nevertheless, more distant polymer layers still serve to decrease the interfacial tension. Exchange of the layers is certainly possible given the fluid nature of this interface. The complex structure of these interfacial layers will be discussed below.

Adsorption of PMA to the Oil–Water Interface

Atactic and isotactic PMA contain slight structural and functional differences from PAA, providing the unique opportunity to explore and compare interfacial properties of each. Both have carboxylic acids as functional groups, but the PMAs have a higher degree of hydrophobicity due to their additional methyl group between the carboxylic acids. Both PMAs exist as a compact coil at low pH and undergo a phase transition between pH 4 and 6 to a more expanded conformation (23–28). Even so, the two PMA isomers exhibit different bulk behavior. Atactic PMA (aPMA) is water soluble in its compact coil conformation whereas isotactic PMA (iPMA) is not. Additionally, the pH-dependent phase transition of aPMA from its extended to more compact conformation upon solution acidification occurs readily, whereas iPMA does not go through this compaction transition upon acidification (23, 25). Instead, acidified iPMA remains in the water soluble extended conformation (25). Because our spectroscopy studies require molecular species to be water soluble, the studies shown below for iPMA were all conducted under acidic conditions where iPMA exists in its more extended water soluble form.

Both forms of PMA are found by VSFS to readily go to the interface and form an ordered polymer layer. As shown in Fig. 4*A*, the carbonyl spectra for both forms of PMA are nearly identical to PAA (Fig. 2). In the methyl region (Fig. 4*B*) the spectra are similar for the two forms of PMA but differ from PAA spectra in this region due to the additional contributions from the methyl groups on the polymer backbone. Nevertheless, analysis of the spectra in the CH region confirms the presence of an oriented backbone for the adsorbed aPMA and iPMA polymers detected. The remarkable similarity in the spectral features for all systems studied indicates that the structural spreading of the polymer at the interface is independent of their different bulk coiled structures, because these structures differ for PAA and both forms of PMA in bulk aqueous solution.

The strong similarity in the VSF spectra observed for the two forms of the PMA polymer suggests that the initial adsorption process does not depend on their isomeric forms and furthermore that the additional hydrophobic methyl group does not have any significant effect on how the carboxylic acid groups or backbone of the polymer conform to the interface. However, complementary surface tension data provide a very different picture. Fig. 5 shows the change in surface tension in the CCl_4/H_2O interface as the two polymers are introduced into the aqueous solution. For aPMA at pH less than 4.5 and concentration of 5 ppm, there is a slow drop in surface tension with time as the polymer increasingly diffuses to the interface. The resulting equilibrium surface tension is measured as 32 mN/m, similar to what is found for PAA at this pH. All results indicate that the adsorption behavior for aPMA is very similar to PAA with the first arriving polymer assembling in a thin and very ordered initial layer followed by additional more randomly coiled polymer snuggling into the interface with time.

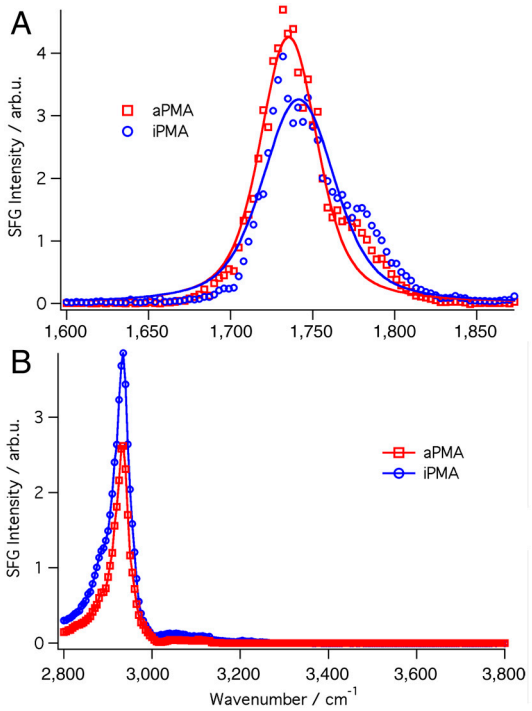

Fig. 4. VSF spectra of PMA in the atactic form (5 ppm, 31.1 kD, red) and reprotonated isotactic form (5 ppm, 3 kD, blue) isomers at pH 1.5. (*A*) VSF spectra of the carbonyl region centered at 1,740 cm^{-1} for iPMA and 1,735 cm^{-1} for aPMA. The solid line is a representative fit of the data. (*B*) VSF spectra of the water and CH region. The dashed line is a guide for the eye.

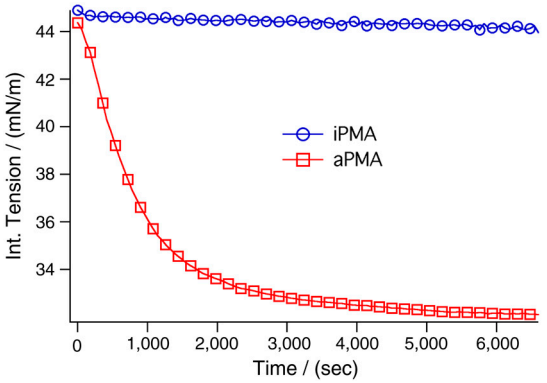

Fig. 5. Interfacial tension measurements of PMA for the atactic (5 ppm, 31.1 kD, red) and reprotonated isotactic (5 ppm, 3 kD, blue) isomers at pH 1.5.

iPMA however shows very different behavior. Upon introduction into solution, there is an immediate small drop in surface tension to 44 mN/m, and this value is nearly invariant with time. The results in this case indicate that unlike the other two polymers, where additional randomly oriented polymers accumulate at the interface, with iPMA, a first thin ordered layer goes onto the interface but further adsorption is not favorable. While both aPMA and iPMA can adsorb to the interface as an ordered layer, the extended nature of iPMA in the bulk phase, in addition to its bulky methyl and carboxylic acid groups, appear to limit further interfacial adsorption. This lack of a slower interfacial adsorption phase for iPMA differs from what is observed for the more compact aPMA and less bulky PAA.

pH Induced Desorption

Both PAA and PMA are weak PEs and therefore in bulk aqueous solution display properties that are highly pH dependent. In general, an increase in pH increases the charge density on both PAA and PMA due to deprotonation of the carboxylic acid groups. For PAA in bulk solution, this increase in charge density causes the polymer to adopt an extended conformation due to charge-charge repulsion between carboxylate functional groups (29, 30). Titrations in this laboratory show the bulk pK_a of PAA to be 6, which is in agreement with literature (31–35). The pK_a value of aPMA, and therefore likely iPMA, is reported to be 7.3 (36). As noted above, an increase in pH for aPMA causes a phase transition from a compact to an extended coil between pH 4 and 6 (23–28). For the experiments conducted here, iPMA has been reprotonated after the phase transition and therefore exists in a more extended conformation in the bulk.

One might expect that added charge and conformational stretching of the polymer at high pH might favor interfacial adsorption. In fact the opposite is dramatically observed in both the VSF and surface tension data. As the pH is raised, desorption occurs over a narrow pH range that is significantly lower than the bulk pK_a in all cases. For both iPMA and aPMA, upon increasing the solution pH to 4.5, the VSF signal in both the CO and CH spectral regions plummet to zero intensity at the same pH, and this lack of signal is constant through pH 10 (see Figs. S1 and S2). This is identical for what we observed for PAA (21). The disappearing CH modes in all cases are replaced by an interfacial spectrum that resembles the spectra obtained in previous studies of the neat CCl_4–water interface (16, 37), where a prominent signal from the free OH stretching mode around 3,700 cm^{-1} appears, corresponding to interfacial water modes and a polymer free interface.

Interfacial tension data support these findings where polymer adsorption is observed as a decline in surface tension between pH 1.5 and 4, but tension then rises from pH 4 to 4.5; interfacial tension reaches a constant value of 44 mN/m, which is very near the neat interfacial tension value of CCl_4–water (38, 39). For PAA, complete desorption occurs over the pH range 4–4.5 and according to the titrations in this laboratory, it occurs at 20% deprotonation of the polymer in bulk, far below the known pK_a. The same trend is observed for both isomers of PMA: They desorb from the interface in the same narrow pH range as that of PAA and desorption occurs well below their pK_a values. Their degree of dissociation is also less than 20% in this pH range according to the literature (40). For weak acids (e.g., carboxylic acid surfactants and phenols) adsorbed at the surface, the pK_a is usually 1–3 units higher than that of the bulk value (41, 42). Given this, the dynamic picture of the interface is one in which less than one in five carboxylic acids along the backbone are deprotonated in order to facilitate desorption of the polymer. While the oriented polymer sections lying at the surface have a higher pK_a than the randomly coiled adsorbed polymer above it, the loops of the surface-adsorbed polymer that protrude into the aqueous phase will be mixed with the randomly coiled polymer above it. This results in simultaneous desorption of both the surface-adsorbed oriented polymer and the randomly coiled polymer that is adsorbed above it. This explains what is happening with PAA as well as aPMA. Even though iPMA only adsorbs to the interface as a thin initial layer with no subsequent layers continuing to build up over time, this layer still desorbs under the same conditions as both PAA and aPMA.

The adsorption and desorption of polymer from the interfacial region is a constant struggle between the free energy; the bulk solubility; the pH of the solution, which dictates the amount of charge on the polymer; and the inherent interfacial activity of the polymer. Depending on the equilibrium conditions of these factors, adsorption to the interface may or may not occur. From a thermodynamic perspective, the desorption of the polymer from the oil–water interface can be thought of in terms of the free energy of desorption, which dictates the energetic cost of moving a functional group from the interface into the bulk. The free energy of desorption for moving a carboxylic acid from the oil–water interface to the bulk water is about +1,630 cal/mol (43). However, deprotonating the acid group significantly lowers the free energy of desorption and thus charged portions of the chain are more easily solvated away from the interfacial region. Due to the polymer being only 20% (or less) deprotonated at the point of observed desorption, the deprotonation of only 1 in 5 carboxylic acids must lower the energy barrier enough to allow the polymer to leave the interface.

For the polymers in this study, why this desorption would occur under such low polymer deprotonation can be explained by several recent studies of bulk PAA behavior. As the pH of the solution is increased and charge accumulates along the length of the polymer, there are cooperative processes that allow a carboxylic acid group neighboring a charge to deprotonate more readily than an acid group that has very little charge surrounding it (30, 44). Such cooperative processes lead to a decrease in the neutral parts of the polymer adsorbed to the interface as the charged sections of the polymer increase in size until the free energy of desorption decreases enough for the entire polymer to become hydrated in the bulk aqueous solution. This is illustrated in Fig. 6, which shows the interfacial region at low and high pH. At low pH the figure depicts the proposed structure of trains adsorbed to the interface while loops are solvated into the aqueous solution, consistent with proposed theoretical pictures (45, 46). These loops contain increasing amounts of charge as pH increases until polymer desorption occurs. Above the oriented polymer adsorbed right at the interface, a subinterfacial region containing randomly coiled polymer that is evidenced by the slower adsorption process in the interfacial tension measurements. This polymer, as seen in the cartoon, has no orientation associated with it, and the time scale during which it adsorbs is much longer than that of the oriented polymer at the interface. The inherent field associated with the oil–water interface acts to orient the polymer at the interface. The field does not penetrate into the water phase enough to orient the subinterfacial polymer, but it is still drawn there due to its interfacial activity. As pH increases to a critical value, the interfacial picture is described by the lower panel, where water structure dominates the interfacial region much like what is seen in a neat CCl_4–water VSFS spectra. The polymers are desorbed from the interface into the aqueous phase and the charged functional groups act to keep the polymer in a stretched out conformation due to charge-charge repulsion (29, 30).

For all PEs examined here the VSFS studies show that only the neutral (protonated) functional groups are observed at the interface even though charged carboxylates are present. The fact that the carbonyl and CH modes of the polymer in the subinterfacial region are not observed indicates that these modes along the polymer backbone do not have a net orientation but instead are in an ensemble of orientations that leads to a net cancellation of VSF signal. This indicates this polymer is most likely in a ran-

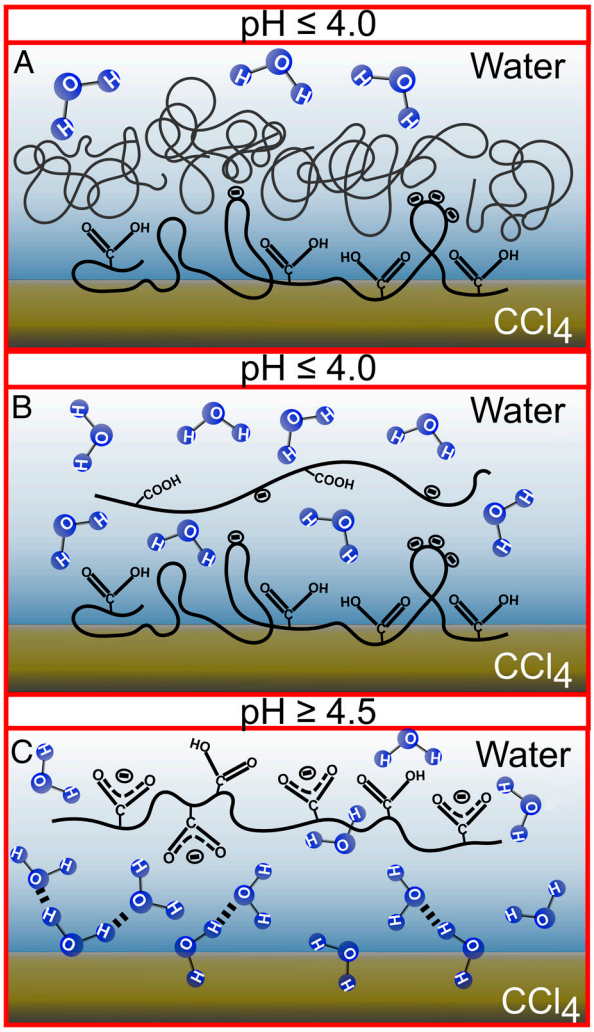

Fig. 6. A cartoon depicting the adsorption and orientation of PAA and PMA at the CCl_4-H_2O interface under different pH conditions. (*A*) Adsorption of PAA and atactic PMA below the critical pH, where randomly coiled polymer continues to adsorb to the subsurface after the initial oriented layer. (*B*) Isotactic PMA where there is an initial highly oriented layer observed, but the stretched out configuration of isotactic PMA prevents continued adsorption to the subsurface. (*C*) The lack of interfacial polymer adsorption and the neat CCl_4-H_2O interface.

domly coiled structure. Right at the interface, the picture consistent with the VSF data is that these carboxylate groups on the polymer must be located on the loops protruding into the water phase and are thus not oriented or near enough to the interface to give VSF signal.

The behavior at the interface is clearly different than what is known about PAA and aPMA in bulk aqueous solution. In bulk aqueous solution the lack of charge-charge repulsion at low pH leads to a random coil of polymer. For aPMA at low charge density the conformation is that of a compact coil made up of several interacting chains with the methyl groups more in the interior and the carboxylic acid groups more on the exterior of the coil (25, 26). This structure has been attributed to several factors including hydrogen bonding, van der Waals interactions, and the hydrophobic effect (24, 27, 40). These studies suggest quite the opposite for the thin layer of PAA and aPMA in the innermost region of the interface. The strong orientation of the carbonyl and CH groups on the polymer at low pH is consistent with a more extended and oriented structure, not the random coiled or compact coil polymer structure found in bulk. A structure consistent with the theory of polymers at soft interfaces is one where the polymer has organized, oriented trains adsorbed at the interface interrupted by loops or coils protruding into the water phase (45, 46). From the spectral data, as the pH (and charge density) increases, the charged carboxylate functional groups do not have a net orientation, as VSF signal was not observed in the 1,400 cm^{-1} region. The accumulated charge on the chain must therefore either be contained in the loops/coils that are solvated by the water, or the charged carboxylates must be positioning themselves to have net opposing orientations along the backbone of the polymer chain in order to have a cancellation of the VSFS signal.

Conclusions

Interfacial structure and adsorption of macromolecules has increasingly proven to play an important role in biological and industrial applications, ranging from protein binding to complexation of nanoparticles and surfactants. Even the most thorough understanding of bulk solution chemistry simply cannot explain much of the chemical behavior of these polymers at interfaces, a location common to many natural and industrial conditions. We found that adsorption of the polymers occurs over two distinct time regimes, the faster of which leads to an initial first layer with highly ordered orientation as a result of the interfacial electric field. The slower step involves adsorption of polymer having no specific order, yet it still adsorbs near the interface due to its interfacial activity. In addition, it was found that desorption of the polymers occurs across a very narrow pH range (*SI Text*) due to a decrease in the free energy of desorption, resulting from the deprotonation of carboxylic acids in the interfacial region.

The implications of this work are twofold. The oil–water interface is a near ideal artifice on which to model the true, in vivo behavior of biomolecules. Not only does it mimic the H_2O-rich environment in which an understanding of the molecule's behavior is most desired, but it also provides the symmetry-breaking which allows for experiment (VSFS in this case) to provide detailed behavioral assay in a setting more realistic than in the bulk. While many polyelectrolytes and biomolecules are well characterized in bulk solution, the conformation, adsorption properties, and dynamics are quite different at interfaces, as shown in this work. For example, recall the abrupt transition between adsorption and desorption at a critical pH is but one such difference clearly not anticipated by results from bulk studies. Other biomolecules, particularly those exhibiting conformational changes, such as protein folding, or enzyme catalysis might well show similar differential behavior. The second implication of this study relates to polyelectrolyte complexation with surfactants and nanoparticles. Studies have found these complexes to be surface active and often attribute this to the surfactant or particle complex. In contrast this work shows that the polyelectrolyte can well be responsible for the increased surface activity (given that both PAA and PMA are surface active by themselves). This insight also stems from the unique environment and properties of the oil–water interface, where the study of macromolecules mimics the true nature of biological and environmental systems.

ACKNOWLEDGMENTS. The National Science Foundation (CHE-065231) has supported the PMA studies. The US Department of Energy, Office of Basic Energy Sciences, Division of Materials Sciences and Engineering under award DE-FG02-96ER45557 has supported the PAA studies.

1. Rebhun M, Meir S, Laor Y (1998) Using dissolved humic acid to remove hydrophobic contaminants from water by complexation-flocculation process. *Environ Sci Technol* 32:981–986.

2. Saito T, Koopal LK, Nagasaki S, Tanaka S (2005) Analysis of copper binding in the ternary system Cu^{2+}/humic acid/geothite at neutral to acidic ph. *Environ Sci Technol* 39:4886–4893.

3. Ramos MA, Fiol S, Lopez R, antelo JM, Arce F (2002) Analysis of the effect of ph on Cu^{2+} fulivc acid complexation using a simple electrostatic model. *Environ Sci Technol* 36:3109–3113.
4. Cooper CL, Dubin PL, Kayitmazer AB, Turksen S (2005) Polyelectrolyte protein complexes. *Curr Opin Colloid Interface Sci* 10:52–78.
5. Jewell CM, Lynn DM (2008) Surface mediated delivery of dna: cationic polymers take charge. *Curr Opin Colloid Interface Sci* 13:395–402.
6. Rosen MJ, Wang H, Shen P, Zhu Y (2005) Ultralow interfacial tension for enhanced oil recovery at very low surfactant concentratioins. *Langmuir* 21:3749–3756.
7. Bowden N, Terfort A, Carbeck J, Whitesides GM (1997) Self-assembly of mesoscale objects into ordered two dimensional arrays. *Science* 276:233–235.
8. Dinsmore AD, et al. (2002) Colloidosomes: Selectively permiable capsules composed of colloidal particles. *Science* 298:1006–1009.
9. Narayan S, et al. (2005) On water: Unique reactivity of organic compounds in aqueous suspensions. *Angew Chem Int Ed Engl* 44:3275–3279.
10. Hore DK, Walker DS, Mackinnon L, Richmond GL (2007) Molecular structure of the chloroform-water and dichloromethane-water interface. *J Phys Chem C Nanomater Interfaces* 111:8832–8842.
11. Hore DK, Walker DS, Richmond GL (2008) Water at hydrophobic surfaces: When weaker is better. *J Am Chem Soc* 130:1800–1801.
12. Moore FG, Richmond GL (2008) Integration or segregation: How do molecules behave at oil-water interfaces. *Acc Chem Res* 41:739–748.
13. Walker DS, Richmond GL (2008) Interfacial depth profiling of the orientation and bonding of water molecules across liquid-liquid interfaces. *J Phys Chem C Nanomater Interfaces* 112:201–209.
14. Walker DS, Moore FG, Richmond GL (2007) Vibrational sum frequency spectroscopy and molecular dynamics simulations of the carbon tetrachloride-water and 1,2-dichloromethane-water interfaces. *J Phys Chem C Nanomater Interfaces* 111:6103–6112.
15. McFearin CL, Richmond GL (2010) The unique molecular behavoir of water at the chloroform-water interface. *Appl Spectrosc* 64:986–994.
16. Scatena LF, Brown MG, Richmond GL (2001) Water at hydrophobic surfaces: Weak hydrogen bonding and strong orientation effects. *Science* 292:908–912.
17. Schrodle S, Moore FG, Richmond GL (2007) In situ invesitgation of carboxulate adsorption at the fluorite-water interface by sum frequency spectroscopy. *J Phys Chem C Nanomater Interfaces* 111:8050–8059.
18. Walker RA, Gruetzmacher JA, Richmond GL (1998) Phosphatidylcholine monolayer structure at a liquid-liquid interface. *J Am Chem Soc* 120:6991–7003.
19. Hore DK, Beaman DK, Parks DH, Richmond GL (2005) Whole molecule approach for determining orientation at isotropic surfaces by nonlinear vibnrational spectroscopy. *J Phys Chem B* 109:16846–16851.
20. Bashforth F, Adams JC (1883) *An Attempt to Test the Theories of Capillary Action* (Cambridge Univ Press, Cambridge, UK).
21. Beaman DK, Robertson EJ, Richmond GL (2011) Unique assembly of charged polymers at the oil-water interface. *Langmuir* 27:2104–2106.
22. Chang TM, Dang LX (1996) Molecular dynamics simulations of CCl_4-H_2O liquid-liquid interface with polarizable potential models. *J Chem Phys* 104:6772–6783.
23. Leyte JC, van der Veen HMRA, Zuiderweg LH (1972) Irreversible potentiometric behavior of isotactic poly(methacrylic acid). *J Phys Chem* 76:2559–2561.
24. Mandel M, Leyte JC, Stadhouder MG (1967) The conformational transition of poly (methacrylic acid) in solution. *J Phys Chem* 71:603–612.
25. Jerman B, Kogej K (2006) Fluorimetric and potentiometric study of the conformational transition of isotactic and atactic poly(methacrylic acid) in mixed solvents. *Acta Chim Slov* 53:264–273.
26. Olea AF, Thomas JK (1989) Fluorescence studies of the conformational changes of poly (methacrylic acid) with ph. *Macromolecules* 22:1165–1169.
27. Nakashima K, et al. (1999) Fluorescence and ftir studies on the ph-dependent conformational change of poly(methacrylic acid) in aqueous solutions. *Bull Chem Soc Jpn* 72:1233–1238.
28. Ruiz-Perez L, et al. (2008) Conformation of poly(methacrylic acid) chains in dilute aqueous solution. *Macromolecules* 41:2203–2211.
29. Katchalsky A, Eisenberg H (1951) Molecular weight of polyacrylic and polymethacrylic acid. *J Polym Sci* 6:145–154.
30. Oosawa F (1971) *Polyelectrolytes* (Marcel Dekker, Inc., New York).
31. Porasso RD, Benegas JC, van den Hoop MAG (1999) Chemical and electrostatic association of various metal ions by poly(acrylic acid) and poly(methacrylic acid) as studied by potentiometry. *J Phys Chem B* 103:2361–2365.
32. Borkovec M, Koper GJM, Piguet C (2006) Ion binding to polyelectrolytes. *Curr Opin Colloid Interface Sci* 11:280–289.
33. Benegas JC, Cleven RF, van den Hoop MA (1998) Potentiometric titration of poly (acrylic-acid) in mixed counterion systems: Chemical binding of cd ions. *Anal Chim Acta* 369:109–114.
34. Gregor HP, Luttinger LB, Loebl EM (1954) Titration of polyacrylic acid with quaternary ammonium bases. *J Am Chem Soc* 76:5879–5880.
35. Cohen-Tannoudji L, et al. (2005) Polymer bridging probed by magnetic colloids. *Phys Rev Lett* 94:038301.
36. Dong H, Du H, Qian X (2009) Prediction of pka values for oligo-methacrylic acids using combined classical and quantum approaches. *J Phys Chem B* 113:12857–12859.
37. McFearin CL, Richmond GL (2009) The role of interfacial molecular structure in the adsorption of ions at the liquid-liquid interface. *J Phys Chem C* 113:21162–21168.
38. Freitas AA, Quina FH, Carroll FA (1997) Estimation of water organic intefacial tensions a linerar free energy relationship of interfacial adhesion. *J Phys Chem B* 101:7488–7493.
39. Apostoluk W, Drzymala J (2003) An improved estimation of water-organic liquid interfacial tension based on linear solvation energy relationship approach. *J Colloid Interface Sci* 262:483–488.
40. Dong J, Tsubahara N, Fujimoto Y, Ozaki Y, Nakashima K (2001) Fourier transform infrared studies of ph- and temperature-dependent conformational changes of solid poly(methacrylic acid). *Appl Spectrosc* 55:1603–1609.
41. Miranda PB, Du Q, Shen YR (1998) Interaction of water with a fatty acid langmuir film. *Chem Phys Lett* 286:1–8.
42. Rao Y, Subir M, McArthur EA, Turro NJ, Eisenthal KB (2009) Organic ions at the air-water interface. *Chem Phys Lett* 477:241–244.
43. Davies JT, Rideal EK (1963) *Interfacial Phenomena* (Academic, New York), 2nd ed..
44. Garces JL, Koper GJM, Borkovec M (2006) Ionization of equilibria and conformational transitions in polyprotic molecules and polyelectrolytes. *J Phys Chem B* 110:10937–10950.
45. Dobrynin AV, Rubinstein M (2005) Theory of polyelectrolyts in solutions and at surfaces. *Prog Polym Sci* 30:1049–1118.
46. Netz RR, Andelman D (2003) Neutral and charged polymers at interfaces. *Phys Rep* 380:1–95.

Supporting Information

Beaman et al. 10.1073/pnas.1200244109

An In-Depth Look at the pH Experiments with PAA and PMA. Detailed plots of the VSF spectra for both PAA and PMA at a variety of pH values are shown in Fig. S1. As described in the main text, clear VSF signal is shown for PAA (*A*), aPMA (*B*), and iPMA (*C*) at low pH values. Raising the solution pH to 4.5 triggers desorption of polymer from the interface in all cases, leaving a nearly neat $H_2O - CCl_4$ (*D*) structure behind. In each of the three panels shown in the carbonyl vibrational stretching region, the amplitudes of the fit peaks are plotted with respect to pH, clearly showing the desorption step. The fit amplitudes (1) of Fig. S1 *A*–*C* plotted as a function of solution pH, are shown in Fig. S2 with fits to the equation,

$$\mathrm{SFG}_A = \mathrm{SFG}_{A_{\min}} + (\mathrm{SFG}_{A_{\max}} - \mathrm{SFG}_{I_{\min}})/(1 + 10^{n(\mathrm{pH}-\mathrm{pK}_a)}) \quad \textbf{[S1]}$$

where n is the Hill coefficient and is an indicator of cooperative ($n \not\approx 1$) or noncooperative ($n = 1$) processes. As shown in Fig. S2, the Hill coefficient (n) for each of the three polymers desorbing from the interface is much greater than 1, indicating that desorption is a highly cooperative process, as one would expect. In addition, the pK_a of each of the polymers is very close to 4, which is significantly lower than what is found in the bulk in literature.

Methods and Materials.

Interfacial Tension. Interfacial tension experiments were carried out on a KSV "Theta" optical tensiometer using the pendant drop method. Drop shape analysis was completed using the KSV supplied software. When acquiring data of aqueous polymer solutions, a neat CCl_4–water interface was always prepared first and the interfacial tension value verified against the known value of CCl_4–water, which is 44 mN/m (2, 3). Once the correct neat interfacial tension value was achieved, then the syringe was filled with the polymer solution of interest and a pendant drop was made. Data was recorded until an equilibrium interfacial tension value was achieved, or in the cases of the long time acquisitions, there was drop failure. Interfacial tension values were calculated from the acquired images using the KSV software.

Spectroscopic Measurements. VSFS data was acquired with an Ekspla laser and IR generation system with a sample area built to accommodate the liquid–liquid cell and inverted beam geometries. This system has been described in detail elsewhere (4). Briefly, a YAG laser outputs 1,064-nm light with ≈30 ps pulse lengths. The 1,064-nm light is split into two lines and one line is frequency doubled to give 532 nm light. A small portion of the 532-nm line is used as the visible portion at the interface, while the remainder of the 532-nm line and the 1,064-nm line are used to generate tunable infrared light via an OPG/OPA/DFG setup. In these experiments, all data was taken with the beams at their respective TIR angles.

Sample Preparation. Chemicals were purchased in the highest purity possible from Sigma-Aldrich (NaOH 1.0 N solution in water, HCl 37%. PAA, also purchased from Sigma-Aldrich, was used as is and the viscosity average molecular weight from the manufacturer was 1,800, 450,000, and 1,250,000 Daltons. aPMA was purchased from Sigma-Aldrich with a viscosity average molecular weight of 31.1 kD and was used as received. iPMA was purchased from Polymer Source and had a viscosity average molecular weight of 3 kD and was used as received. Solutions were prepared using clean glassware, an analytical balance and water from a Barnstead ePure system. Solution pH was adjusted using NaOH or HCl and tested using EMD pH paper with regular verification via an Oakton 110 series pH meter.

The sample cell was designed from a solid piece of Kel-f and contains two windows set normal to the incident and outgoing 532-nm beam and are sealed with Dupont Kalrez® perfluoropolymer O-rings. The input window was CaF_2 and the output window was BK-7 glass. All glassware, the cell, the BK-7 window, and the O rings were soaked in concentrated sulfuric acid with NoChromix for a minimum of 12 h and then each piece was rinsed with 18 MΩ water from a Barnstead ePure filtration system for at at least 25 min. The CaF_2 window was allowed to soak in the same acidic solution for 15–20 min and then copiously rinsed.

Data acquisition started immediately after the interface was prepared. Each spectra shown in these experiments is an average of at least 300 laser shots per data point. Long term equilibration was checked by letting the interface sit for several hours and then retaking the spectra. Unless otherwise noted, long term equilibration was not observed.

1. Beaman DK, Robertson EJ, Richmond GL (2011) Unique assembly of charged polymers at the oil-water interface. *Langmuir* 27:2104–2106.
2. Freitas AA, Quina FH, Carroll FA (1997) Estimation of water organic intefacial tensions. A linerar free energy relationship of interfacial adhesion. *J Phys Chem B* 101:7488–7493.
3. Apostoluk W, Drzymala J (2003) An improved estimation of water-organic liquid interfacial tension based on linear solvation energy relationship approach. *J Colloid Interface Sci* 262:483–488.
4. McFearin CL, Richmond GL (2009) The role of interfacial molecular structure in the adsorption of ions at the liquid-liquid interface. *J Phys Chem C* 113:21162–21168.

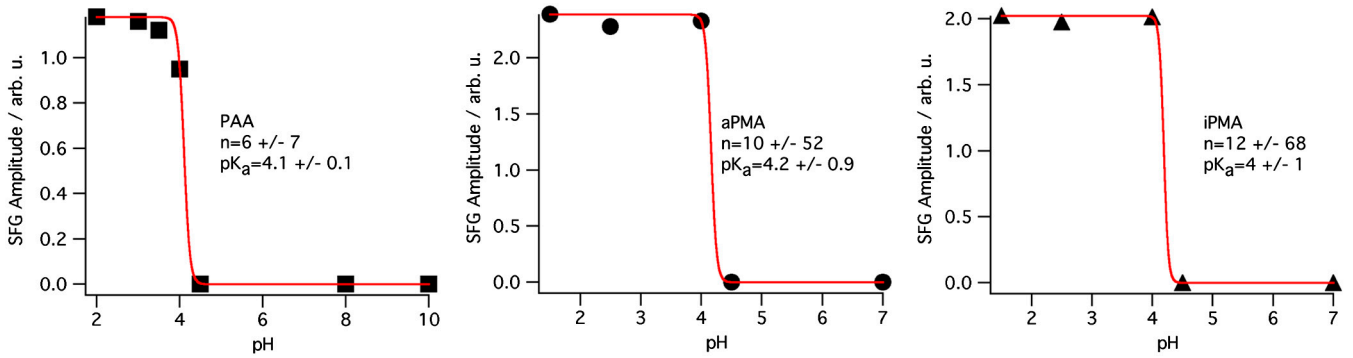

Fig. S1. Plots of SFG amplitude from the pH seris for PAA, aPMA, and iPMA fit to S1.

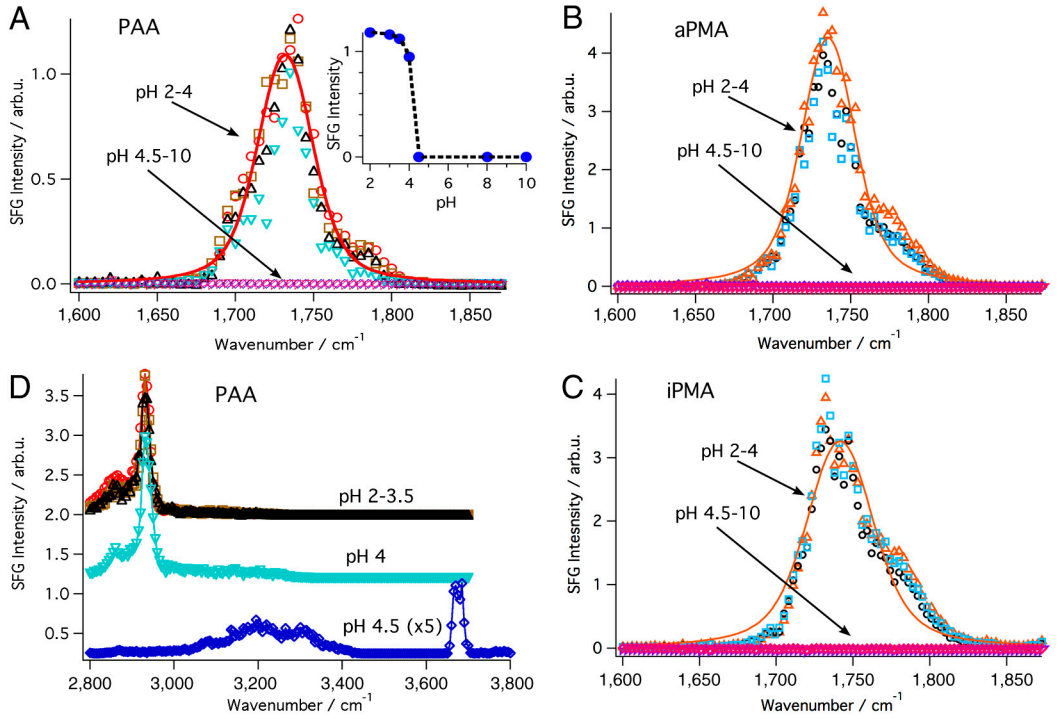

Fig. S2. VSF spectra of PAA and PMA at the CCl_4–water interface as a function of pH. (*A*) VSF spectra of the PAA (5 ppm, 450 kD) carbonyl stretch at 1,732 cm^{-1} for pH 2–10. The solid line is a representative fit of the data. The inset shows the plotted amplitudes obtained from the global fit as a function of pH. The dashed line is a guide for the eye. (*B*) VSF spectra of the carbonyl stretch for atactic PMA from pH 2–10. (*C*) VSF spectra of the carbonyl stretch for isotactic PMA from pH 2–10. (*D*) VSF spectra of the water and CH region of an aqueous PAA–oil interface for pH 2–4.5 (spectra are offset for clarity).